Available online at www.sciencedirect.com
SCIENCE DIRECT®
Journal of Membrane Science 241 (2004) 95–103
journal of MEMBRANE SCIENCE
www.elsevier.com/locate/memsci

Preparation and characterization of non-supported microfiltration membranes from aluminosilicates

M.C. Almandoz [a], J. Marchese [a,b,*], P. Prádanos [b], L. Palacio [b], A. Hernández [b]

[a] *Laboratorio de Ciencias de Superficies y Medios Porosos, CONICET-FONCyT, Universidad Nacional de San Luis, San Luis 5700, Argentina*
[b] *Grupo de Superficies y Materiales Porosos, Dpto. de Termodinámica y Física Aplicada, Facultad de Ciencias, Universidad de Valladolid, Valladolid, Spain*

Received 16 January 2004; received in revised form 21 January 2004; accepted 30 March 2004

Abstract

In the present work non-supported microfiltration ceramic membranes have been made from different aluminosilicate paste formulations. The cast green dopes were sintered at temperatures between 1100 and 1400 °C. The membrane characterisation was made by scanning electron microscopy (SEM), mercury porosimetry, gas and water permeabilities and microorganisms rejection. The results indicate that an appropriate election of the size of the particles in the paste and of the final sintering temperature allows to obtain membranes with different mechanical and structural properties, with mean pore sizes within the range from 0.1 to 1 μm, that make them suitable for microfiltration.

Keywords: Ceramic membranes; Microfiltration; Membrane characterization; Aluminosilicates

1. Introduction

Nowadays membranes manufactured for microfiltration (MF) can be composites, symmetric and asymmetric made from polymeric or inorganic materials. They can be, also manufactured with different geometric configurations: tubular, flat, monolithic, etc.

The active layer, which controls the process, of a ceramic membrane for liquid permeation consists of a porous layer, usually symmetric, with a pore density of 10^9 pores/cm^2 approximately and a porosity (or void volume fraction) between 30 and 70%. The pore size is included in a range of 50–1000 nm in the case of MF and 2–50 nm for ultrafiltration (UF) membranes [1].

Ceramic membranes can be made by classical techniques using suspensions of powder materials and/or by the sol–gel technique by using hydrated oxides salts as precursors (colloidal suspension route) or by the employ of alkoxides (polymeric gel route). Anderson et al. [2] describe the synthesis of γ-AlOOH xerogel from tri sec-butoxide of alumina. When the obtained colloidal boehmite is sintered at temperatures over 1000 °C it is converted to the very stable chemical form of α-Al_2O_3, with a mean pore size of 80 nm suitable for MF process.

Cot et al. [3] prepared active layers of ZrO_2 membranes from zirconium alkoxide. The ZrO_2 membrane is manufactured on a support layer of alumina by using a casting process. The pore size of these membranes increases with temperature, from 6 nm (700 °C) to 70 nm (1200 °C). The preparation of TiO_2 membranes, both supported and non-supported, is described by several authors [2,4–7]. Cot et al. [3] made also TiO_2 membranes with pores from 6 nm (500 °C) to 180 nm (1100 °C). These high temperature calcined TiO_2 membranes fall in the MF range.

Larbot et al. [8] have described the synthesis process of silica membranes from a mixture of colloidal silica. They obtained pore sizes from 6 to 10 nm for temperatures between 400 and 800 °C. Gallagher and Klein [9] synthesized non-supported flat sheets (around 100 μm in thickness) of SiO_2 with big pores of 30 micrometers. Lee et al. [10] obtained alumina films of MF-UF prepared by the sol–gel method with suitable strength and resistance to the corrosion.

At present, there are not many works describing the preparation of MF membranes from ceramic powder suspensions. Pei Wang et al. [11] manufactured ceramic supported MF membranes by using α-Al_2O_3 powder with mean particle size from 0.5 to 2.8 μm. MF layers were prepared with pore

* Corresponding author. Tel.: +54 2652 436151; fax: +54 2652 430224.
E-mail address: marchese@termo.uva.es (J. Marchese).

0376-7388/$ – see front matter © 2004 Elsevier B.V. All rights reserved.
doi:10.1016/j.memsci.2004.03.045

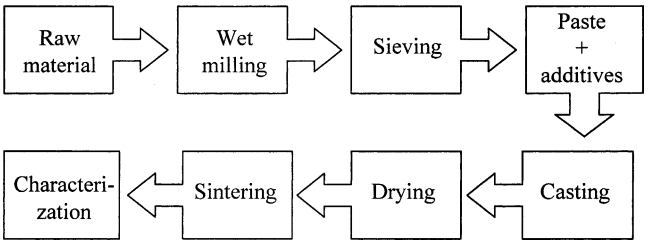

Fig. 1. Diagram of the active layers preparation.

sizes in the 0.08–0.8 μm range, depending on particle size of the paste and the sintering temperature (900–1327 °C). Shi-Hee Lee et al. [12] prepared MF layers with pore sizes from 0.2 to 0.3 μm from α-Al_2O_3 slurries (mean particle size of 0.4 μm) on a tubular composite support of alumina.

In this work, it is proposed the preparation of ceramic active layers for liquid microfiltration by using suspensions of aluminosilicate powder. Here, the overall particle size in the green dope is controlled by changing its composition. The raw materials employed were easily obtainable at low costs, as clay, kaolin, alumina, quartz and calcium carbonate. The effect of particle size distribution, density and viscosity of the ceramic paste and the drying and sintering process on the structure and active layer morphology have been analysed.

2. Experimental

2.1. Membrane preparation procedure

The general procedure employed in the preparation of the different substrates of the active layer was casting the suspension by using aluminosilicate powders and other raw materials. The manufacture process includes the following main steps [13,14] (Fig. 1): (a) paste formulation from the raw materials, (b) paste conditioning (milling, sieving and suspension stabilization), (c) paste casting and (d) drying and sintering.

2.1.1. Raw materials and paste formulation

2.1.1.1. Ball clay. The Argentinean company Piedra Grande provided the clays used in the present work. The chemical composition was determined by Induction Coupled Plasma (ICP) and Atomic Absorption with Graphite Furnace (AA-GF), with weight percentages of: 61% SiO_2; 25% Al_2O_3; 0.7% Fe_2O_3; 1.6% Oca; 0.45% MgO; 0.5% TiO_2; 1.1% K_2O; 0.15% Na_2O and a 9.5% of solids lost by calcination. These clays have an important content of alkalis that reduce their melting point. The mean particle size is 2.7 μm. The fine particles and the organic material present in the clay give plasticity to the green paste.

2.1.1.2. Kaolin. It was provided also by Piedra Grande company (Argentina). The chemical composition determined by ICP and AA-GP is, given in weight percentage: 52% SiO_2; 30% Al_2O_3; 0.4% Fe_2O_3; 0.25% TiO_2; 0.6% CaO; 0.1% MgO; 1.4% K_2O; 0.45% Na_2O and a 14.8% of solids lost by calcination. The particle mean size is 3.2 μm. The kaolin provides to the paste low plasticity and high refractory properties.

Table 1
Paste formulations

Raw materials	Formulation (% (w/w))			
	Paste P1	Paste P2	Paste P3	Paste P4
Clay	20	20	15	15
Alumina	10	25	30	50
Kaolin	40	35	30	–
Calcium carbonate	–	–	9	13
Quartz	29	19	14	20
Additives (sodium carbonate, sodium hexametaphosphate, tannic acid)	1	1	2	2

2.1.1.3. Quartz. It was provided by Piedra Grande Company (Argentina). SiO_2 was present in a 96–98% (w/w). It also contains low quantities of Al_2O_3 (0.5–1% (w/w)) and alkalis (0.1–0.3% (w/w)). The particle sizes range from 1 to 60 μm.

2.1.1.4. Alumina. Obtained from bauxite by the so-called complex process Bayer and provided by Alcoa S.A. (Argentina). Typically it contains more than a 98% (w/w) of Al_2O_3, 0.5–1% (w/w) Na_2O and 0.05–0.07% (Fe_2O_3 + SiO_2). The particle size analysis by ASTM mesh sieving showed that the 90% of the material was from 100 to 180 μm.

2.1.1.5. Calcium carbonate. With a chemical analytical purity (p.a.) as determined by ACS. The particle size is between 30 and 80 μm as determined by ASTM mesh sieving.

Paste formulations are shown in Table 1, expressed in (w/w) percentage. In general, in order to increase the pore size, the percentage of kaolin and clay were decreased while the alumina content was consequently increased. Four green pastes or suspensions, identified as P1, P2, P3 and P4, were prepared by adding the raw materials into distillated water (50% (w/w)) with rapid stirring during 2 h to achieve homogeneous solution.

2.1.2. Green dope preparation

One of the main factors to control the porosity and pore size of the ceramic membranes is the particle size. The P1, P2, P3 and P4 green pastes suffered a wet milling process during 2 h, using a mill, Retsch-PM4000, at a constant speed of 200 r.p.m. Afterwards they were sieved through a mesh 400 ASTM (particle size < 40 μm). The particle size distribution was measured by a Micromeritics SediGraph 5100 apparatus.

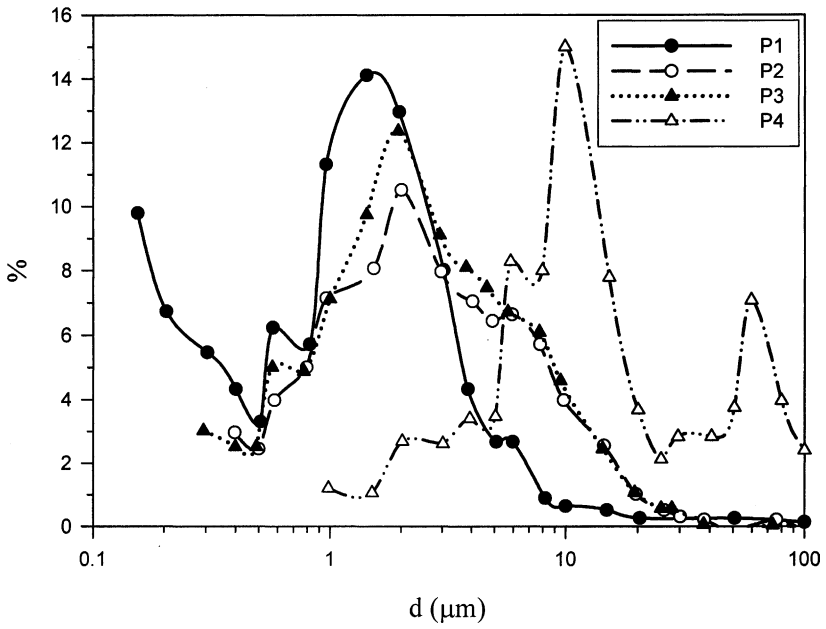

Fig. 2. Particle diameter distribution for the prepared pastes.

Prior to the casting process, the paste must have the appropriated density and viscosity. Thus different additives were aggregated (anhydrous Na_2CO_3 purity grade 99.5%; tannic acid p.a., sodium hexametaphosphate p.a.) that give, also, a good paste dispersion, homogeneity and plasticity. Specifically, Na_2CO_3 and tannic acid act as colloid protectors and deflocculants improving dispersion properties. While sodium hexametaphosphate decreases the viscosity and tixotropy of the pastes. These additives were added to the milled and sieved stirred suspensions and then, after 12 h, the paste was kept without stirring for 2 days (paste ageing). The density was determined with a digital density/specific gravimeter and the viscosity measured by a digital viscometer, Brookfield-DVIII.

2.1.3. Paste casting

Ceramic active layers were moulded by a casting method. Plaster moulds, once flooded with the green dope, absorb water and leads to a surface flocculation of the paste particles due to calcium sulphate. Three different mould configurations were used:

- Circular-flat, with a 0.0254 m of diameter and 0.0025 m of thickness.
- Prism with a square section, 0.2 m long and 0.015 m width and for the thickness.
- Tubular 0.3 m long and 0.012 m of diameter.

2.1.4. Drying and sintering of green substrate

The crude ceramic elements were slowly dried at environmental temperature during 12 h and then were put in a mechanical convection oven which temperature increased sequentially, 10 °C every 30 min from 50 to 110 °C. Neither cracks nor fissures were detected.

Sintering process was done in a furnace, Nabertherm-Ceramotherm N200 with an automatic temperature controller. In order to avoid the appearance of cracks during both the α–β transition of quartz (573 °C) and the calcination of $CaCO_3$ (537 °C), two temperature ramps were used during heating. The first one up to 600 °C with a 5 K/min speed; in the second ramp the heating speed was higher (10 K/min) to the sintering temperature. This temperature was then kept constant for 30 min. In order to determine the effect of the final sintering temperature (T_s) on the structural-functional properties of the active layers, several experiments were done with $T_s = 1100$, 1200, 1300 and 1400 °C. The obtained membranes were identified as M4, M3, M2 and M1, corresponding to pastes P4, P3, P2 and P1, respectively.

Table 2
Some physical characteristics of the pastes

Physical parameters	P1	P2	P3	P4
Particle mean diameter (μm)	0.97	2.18	2.33	10.79
Density (g/cm^3)	1.49	1.46	1.54	1.64
Viscosity (5–50 rpm) (cP)	6000–600	7000–1000	6500–600	7000–1000
Tixotropy index (cP/s)	20,700	25,000	27,000	31,600

2.2. Membrane characterisation

The membranes were characterised by studying both their structure and functionality. Structure was studied by scanning electron microscopy (SEM), mercury porosimetry and flexion resistance. Their functionality were analysed by gas permeability, water flux and solute rejection experiments.

Samples were covered with a thin gold layer by sputtering and SEM images of these membranes were obtained by using a JEOL (JSM-T300) at a 750× magnification. Mercury porosimetry was carried out using an Autopore III 9410 porosimeter, working from 0 to 414 MPa, corresponding to a pore sizes from 300 to 0.003 μm. Finally, the mechanical resistance to a flexion or the called breaking module, was determined with a Comten apparatus, model 942KVC1000. The test was made according DIN 51030 norms, using ceramic rectangular patterns subjected to the same velocity of charge (10 cm/min).

The total flux of gas through the pores of the active layers of the samples with a circular-flat geometry ($T_s = 1200\,^{\circ}C$) was measured using the permeation equipment described elsewhere [15]. To determine the hydraulic permeability and the corresponding radius, water flux was measured with the tubular membranes. The effective permeation area was $7.85 \times 10^{-3}\,m^2$ and the membrane thickness was 0.001 m of wall thickness. The corresponding water flux was determined for transmembrane pressures (Δp) between 0 and 70 kPa, in classical permeation equipment for liquids [16].

On the other hand, solute rejection experiments have been made with tubular membranes manufactured at 1200 °C, using hydraulic permeability standard equipment. The feed consist of an aqueous solution with a microbial charge around 100 millions of Aerobic Colony Counts per millilitre of effluent also known as the total viable count (TVC) and 48 millions of total coliform bacteria per millilitre. The average size of such microrganisms is mainly determined by *Escherichia Coli* and Proteus with stick shapes and minimal thickness in the range from 0.5 to 1 μm. The sample was fed in the inner duct of the tubular membrane with a peristaltic pump. The feed and permeation solutions were characterised by microbial analysis described in the Standard Methods for the Examination of Water and Wastewater [17].

3. Results and discussion

3.1. Properties of the pastes

Fig. 2 shows the particle size distribution for the pastes prepared. It can be seen that paste P4 has a centred distribution for bigger values than the rest of the samples; that is due to its high percentage of alumina, calcium carbonate and quartz (see Table 1). The rest of the pastes showed relatively wide distributions with maximums, which are similar to the original distribution for the clay and kaolin. Table 2 summarises the particle mean size for the different samples.

The time evolution of viscosity was measured at 25 °C with a constant rotation velocity of the spindle (20 rpm). The dependency of viscosity with rotation velocity was measured by taking the resulting viscosity after 10 min for velocities from 5 to 50 rpm. Fig. 3 shows the obtained data for the P4 sample. From these results, it can be seen that viscosity decreases with time for a constant shear stress (tixotropic fluid). A decreasing viscosity with increasing speeds (pseudoplastic behaviour) can also be seen. When the rotation speed decreases, viscosity is higher than previous, the area between both the curves gives a measurement of the tixotropy index (I) of the fluid. Similar behaviours were obtained for P1, P2 and P3. The obtained results for the tixotropy index (I) for all the pastes can be found in Table 2. Density results (ρ), as obtained with the digital density/specific gravimeter, are also shown.

3.2. Structural characterization of membranes

Fig. 4 shows SEM cross-section images of M1, M2 and M3 membranes for different sintering temperatures. These cross-section images show a symmetric morphology, with

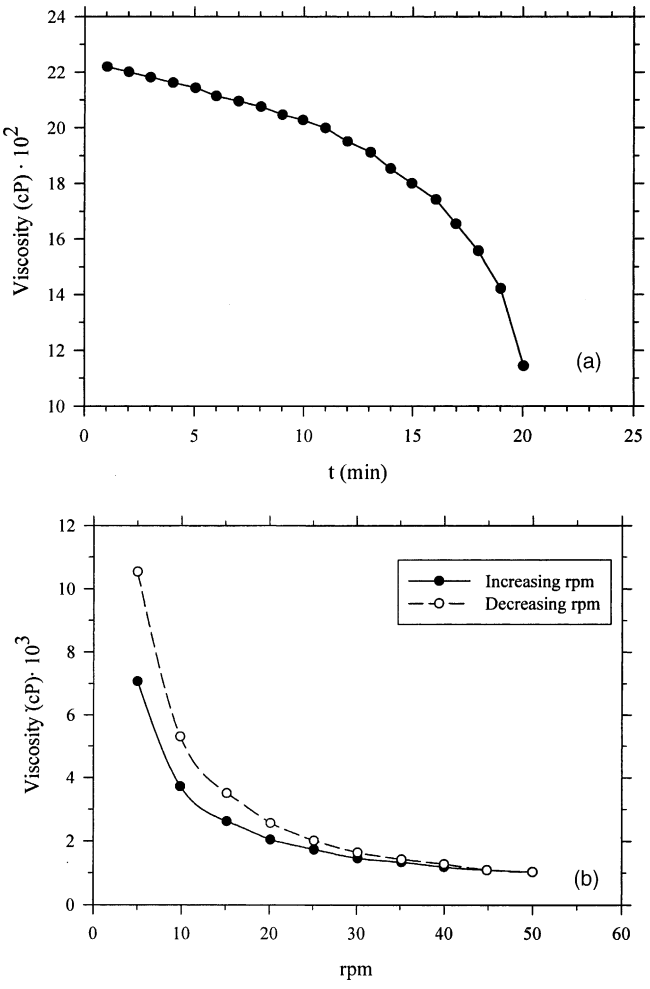

Fig. 3. Viscosity for the P4 paste vs. (a) time and (b) the rotation speed.

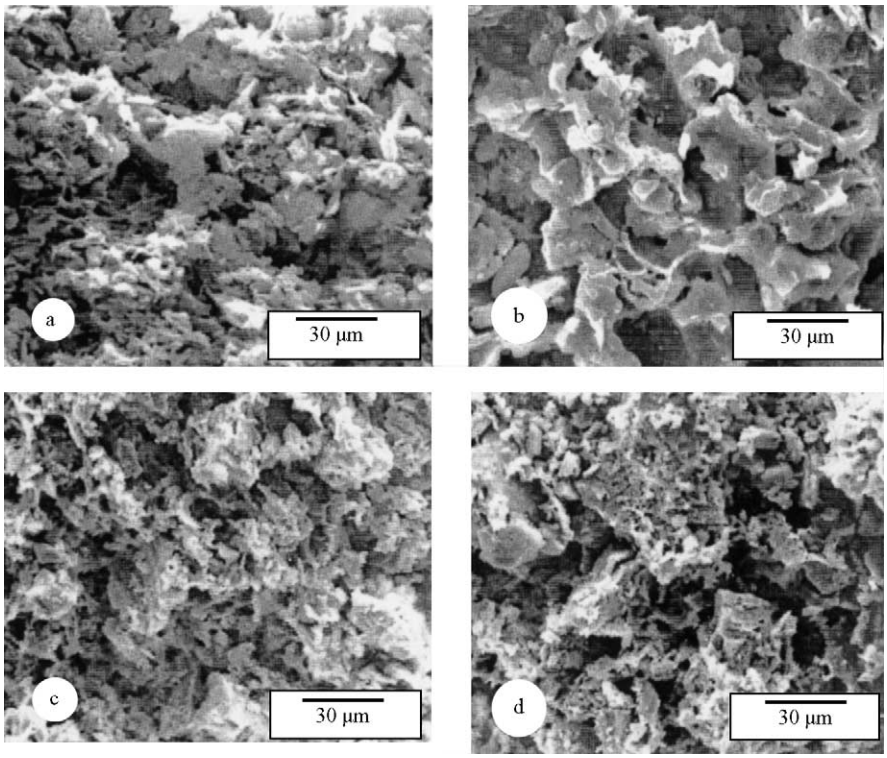

Fig. 4. SEM images of membrane cross-sections (750×) for: (a) M1, $T_s = 1100\,^{\circ}C$; (b) M1, $T_s = 1300\,^{\circ}C$; (c) M2, $T_s = 1200\,^{\circ}C$; (d) M3, $T_s = 1200\,^{\circ}C$.

big granules (alumina) and smaller laminated particles (clay and kaolin) bound each other, forming the fundamental skeletal structure of the alumina–silica. The aggregates of alumina, quartz and alkali allowed the consolidation of the structure of the ceramic body. The calcium carbonate, besides its action reducing melting point, contributes to form bigger pores and increases the total porosity of the membrane (M4 and M3) due to CO_2 formation during the sintering process. In all the cases the membranes showed a surface with rough morphological structure. The ceramic substrates sintered at 1100 °C show free particles (Fig. 4a), which indicate that this temperature is not high enough to obtain an adequate sintering and consolidation of the structure. For $T_s = 1200\,^{\circ}C$ the structure is more consolidated (Fig. 4c and d). While for sintering temperatures over 1300 °C the particles melt together giving smaller cavities

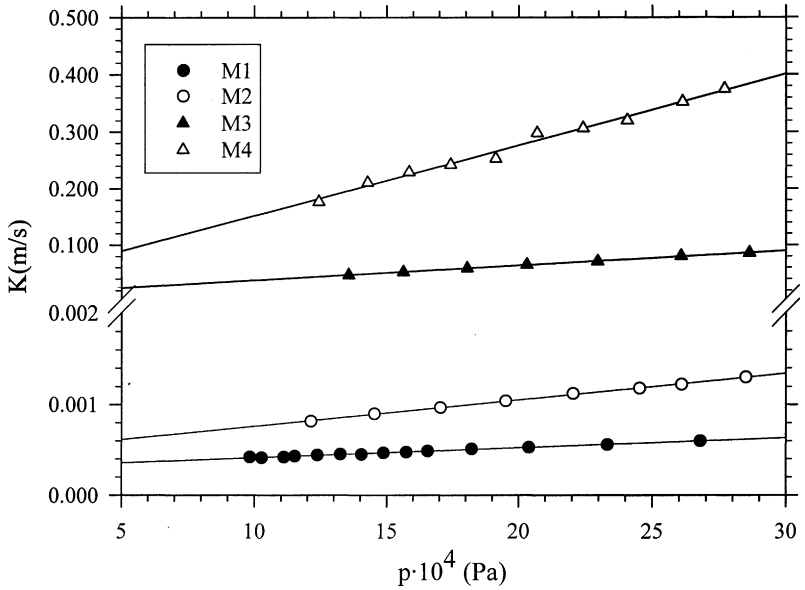

Fig. 5. N_2 gas permeability vs. mean pressure for the membranes sintered at 1200 °C.

Table 3
Structural parameters for the membranes sintered to 1200 °C, by gas permeability and mercury porosimetry

Membrane	Gas permeability		Mercury porosimetry		
	$r_g \pm$ error (μm)	ε/q^2	$r_{Hg} + \sigma$ (μm)	Skeletal density (g/cm^3)	ε (%)
M1	0.043 ± 0.005	0.068	0.13 + 0.08	2.90	35
M2	0.093 ± 0.007	0.065	0.19 + 0.09	2.77	41
M3	0.356 ± 0.011	0.459	0.55 + 0.22	2.75	45
M4	0.463 ± 0.010	0.647	1.10 + 0.46	2.44	46

(Fig. 4b). At a given sintering temperature, the sizes of the particles increase in the series M1, M2, M3 and M4, according to their different formulations.

From gas permeability results, the pore mean radio (r_g) of the membrane can be obtained from the total effective permeability of gas (K, m/s) by, [15]

$$K = 2.133\frac{r_g v}{l}\frac{\varepsilon}{q^2} + 1.6\frac{r_g^2}{l\eta}\frac{\varepsilon}{q^2}p \quad (1)$$

The first term on the right corresponds to the slipping flux, being v the molecular mean velocity of the permeant, q the tortuosity, (ε/q^2) the effective porosity and l the membrane thickness. The last term is the viscous flux where p is the mean pressure and η the gas viscosity. For a given membrane, Eq. (1) shows that, except K and p, the rest of the values are constant. So, a graph for K versus p should give a straight line with intercept A and slope B, which correctly combined let us to get the r_g value as

$$r_g = 1.333\frac{B}{A}\eta v \quad (2)$$

Gas permeability measurements were made by using nitrogen at $T = 303$ K; in these conditions $v = 478.4$ m/s and $\eta = 1.79 \times 10^{-5}$ Pa s. Fig. 5 shows the experimental results for permeabilities. The pore mean size and effective porosity for the membranes are shown in Table 3.

Fig. 6 shows the pore size distribution curves corresponding to mercury porosimetry measurements for the membranes with a flat geometry and sintered to 1200 °C. The main structural parameter data are summarized in Table 3. These results show that pore size decreases with the particle mean size of the pastes. Membranes M1 and M2 have narrow distributions with only a significant peak. On the other hand M3 and M4 show a clear bimodal distribution with lower pore sizes.

3.3. Membrane functional characterization

Hydraulic permeabilities, L_h, were evaluated from the slopes of the water flow through the membranes versus pressure graphs according to Hagen–Poiseuille

$$J = \frac{n\pi r^4 \Delta p}{8\mu l} = L_h \Delta p \quad (3)$$

where J (m/s) is the flow density of permeated water, n the pore density (number of pores per m^2), μ the water viscosity, l the pore length (≈10^{-3} m). By using the porosity $\varepsilon = n\pi r^2$ in Eq. (3), the corresponding pore radius can be obtained

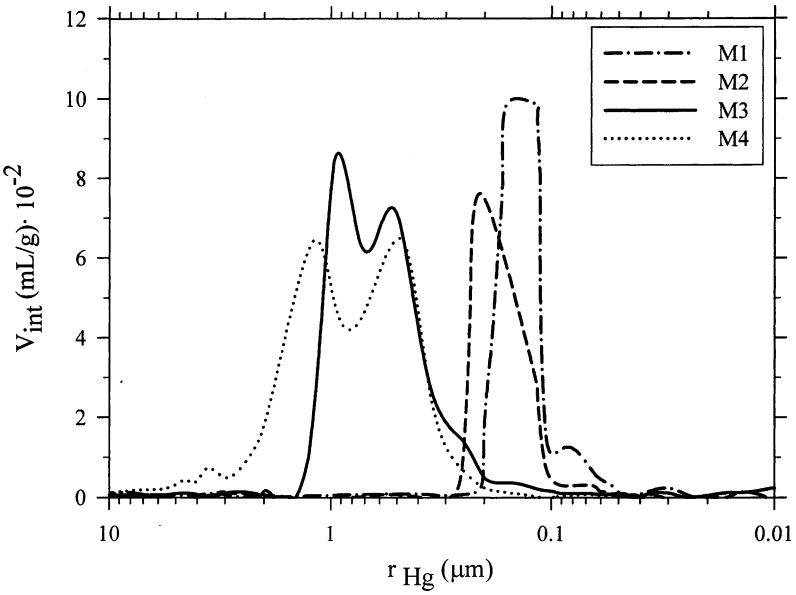

Fig. 6. Pore size distribution for M1, M2, M3, and M4 ($T_s = 1200$ °C) by mercury intrusion.

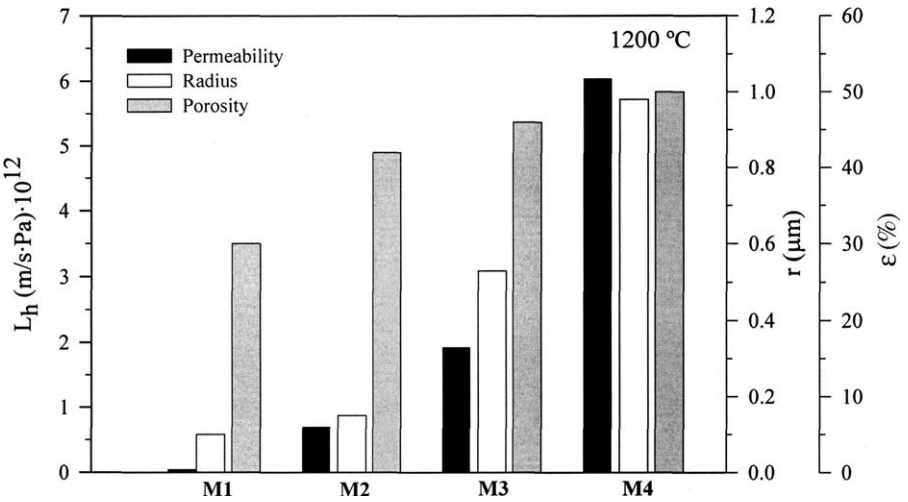

Fig. 7. Hydraulic permeability, porosity and the corresponding radius for the membranes sintered at 1200 °C.

from

$$r = \left[\frac{8\eta l}{\varepsilon} L_h\right]^{1/2} \quad (4)$$

where ε was determined by the pycnometric method, by using water as wetting liquid. Fig. 7 shows the evaluated values for the L_h and ε for each membrane prepared to 1200 °C. Equal behaviour was found for the other temperatures. The effect of the sintering temperature is shown in Fig. 8 for M3 membrane. Also, very similar effects of sintering temperature are found for the other membranes.

These figures show that radius and permeability increase considerably with increasing particle size, whereas porosity increases only slightly. On the other hand, an increment in the sintering temperature produces an almost linear decrease, for the analysed magnitudes. This can be attributed to a high densification of the porous structure when the membranes are sintered at higher temperatures.

When the results for the pore mean radii (obtained by the different techniques) are compared, several discrepancies can be seen. It is reasonable that gas permeability gave smaller pore radii as far as gas can permeate through smaller pores than water or mercury. Mercury porosimetry gives bigger pores because it detects non-only actual pores but other non-interconnected voids of the porous matrix. The most appropriate values are those obtained by hydraulic permeability because they are directly related with the liquid flux for microfiltration process.

Fig. 9 shows the rejection coefficient (R) as a function of the mean size pore for the membranes sintered at 1200 °C, as obtained from water permeability. The coefficients were

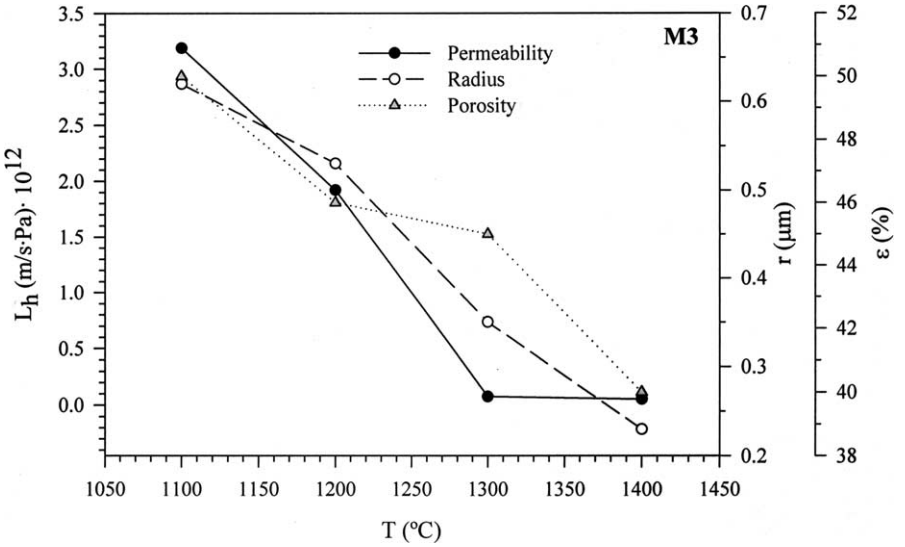

Fig. 8. Hydraulic permeability, porosity and the corresponding radius for the M3 membrane versus the sintering temperature.

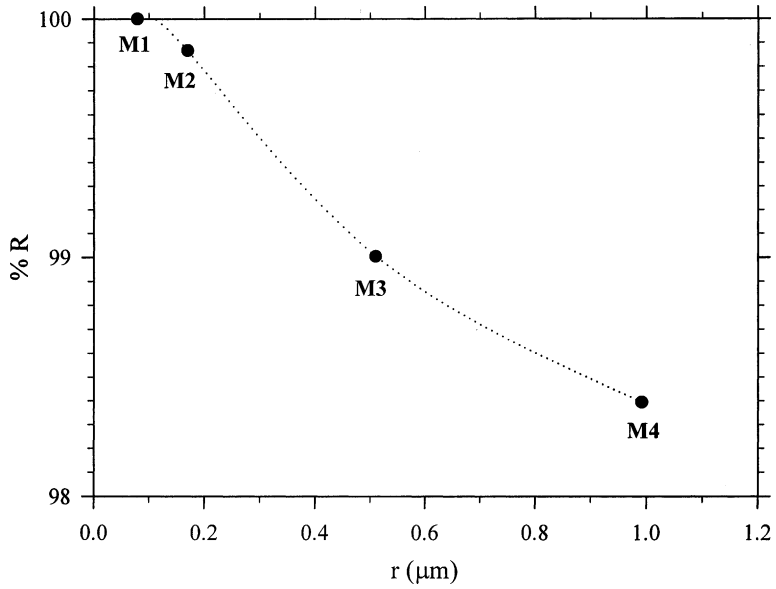

Fig. 9. Microorganisms rejection for the different membranes ($T_s = 1200\,^{\circ}C$).

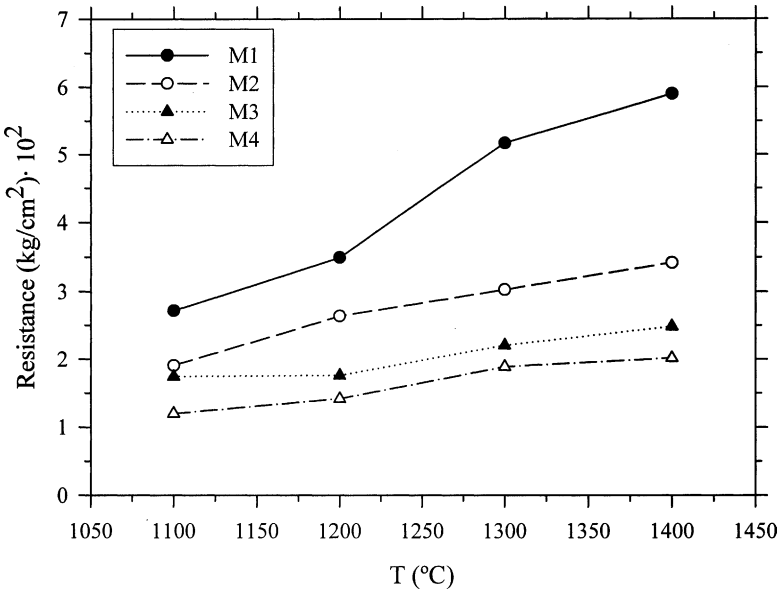

Fig. 10. Resistance to flexion as a function of the sintering temperature.

evaluated from

$$R\,(\%) = \left(1 - \frac{C_p}{C_0}\right) \times 100 \qquad (5)$$

where C_p and C_0 are the bacteria concentration (TVC) for the permeate and the feed, respectively.

These results show clearly that the selectivity of the membranes is high, with a microorganisms rejection bigger than 90% in all cases, reaching 100% values for the M1 membrane.

3.4. Mechanical properties

The obtained resistance to flexion is shown in Fig. 10. As it was expected, an increase in the sintering temperature increases resistance due to a decrease in the volume void fraction linked to a densification of the membrane (see Fig. 8).

4. Conclusions

The adequate formulation of the ceramic pastes, with different proportions of clay, alumina, quartz, calcium carbon-

ate and additives, allowed to sinter different active layers suitable for microfiltration membranes and as intermediate support layer for ultrafiltration membranes prepared by the sol–gel process.

In this study the heating velocity in the sintering process to get active layers free of cracks and fissures has been established. An increase in temperature of sintering leads to a higher density and mechanical resistance, along with a smaller pore volume of the membranes. The structures were symmetric, consisting of laminar particles and granules with crystalline aspect binding each other, forming an skeletal vitrified structure, with holes or pores.

It has been shown that the optimum sintering temperature is between 1200 and 1300 °C. Lower temperatures give low consolidated structures for the ceramic material, while higher temperatures produce a collapse in the porous structure and a consequent considerably lower the hydraulic permeability.

Acknowledgements

Part of this work was granted by the Spanish Secretaría de Estado de Educación y Universidades (SAB2001-0107), to Plan Nacional IDI (PPQ2002-02305, MAT2002-00178 and MAT2000-0506-P4 03), to Junta de Castilla y León (VA021/03 and VA022/03), to Consejo Nacional de Investigaciones Científicas y Técnicas de Argentina (PIP 054/98), and Agencia Nacional de Promoción Científica y Tecnológica (PICT 14-09760).

References

[1] R. Bhave, Inorganic Membranes Synthesis, Characteristics and Applications, Van Nostrand Reinhold, New York, 1991.
[2] M.A. Anderson, M.J. Gieselman, Q.Y. Xu, Titania and alumina ceramic membranes, J. Membr. Sci. 39 (1988) 243–258.
[3] A. Larbot, J.P. Fabre, C. Guizard, L. Cot, Inorganic membranes obtained by sol–gel techniques, J. Membr. Sci. 39 (1988) 203–212.
[4] A.J. Burggraaf, K. Keizer, B.A. Vanhassel, Ceramic nanostructure materials membranes and composite layers, Solid State Ionics 32 (3) (1989) 771–782.
[5] V.T. Zaspalis, W. Vanpraag, K. Keizer, J.G. Vanommen, J.R.H. Ross, A.J. Burggraaf, Reactor studies using vanadia modified titania and alumina catalytically active membranes for the reduction of nitrogen-oxide with ammonia, Appl. Catal. 74 (1991) 249–260.
[6] M.J. Gieselmann, M.A. Anderson, M.D. Moosemiller, C.G. Hill, Physico-chemical properties of supported and unsupported α-Al_2O_3 and TiO_2 ceramic membranes, Separ. Sci. Technol. 23 (1988) 1695–1714.
[7] L. Palacio, P. Prádanos, J.I. Calvo, G. Kherif, A. Larbot, A. Hernández, Fouling, structure and charges of a composite inorganic microfiltration membrane, Colloid Surf. A 138 (1998) 291–299.
[8] A. Larbot, J.P. Fabre, C. Guizard, L. Cot, J. Gillot, New inorganic ultrafiltration membranes—titania and zirconia membranes, J. Am. Ceram. Soc. 72 (1989) 257–261.
[9] D. Gallagher, L.C. Klein, Silica membranes by the sol–gel process, J. Colloid Interf. Sci. 109 (1986) 40–45.
[10] J.W. Lee, C.W. Won, B.S. Chun, H.Y. Sohn, Dip coating of alumina films by the sol–gel method, J. Mater. Res. 8 (1993) 3151–3157.
[11] P. Wang, P. Huang, N.P. Xu, J. Shi, Y.S. Lin, Effects of sintering on properties of alumina microfiltration membranes, J. Membr. Sci. 155 (1999) 309–314.
[12] S.H. Lee, K.C. Chung, M.C. Shin, J.I. Dong, H.S. Lee, K.H. Auh, Preparation of ceramic membrane and application to the crossflow microfiltration of soluble waste oil, Mater. Lett. 52 (2002) 266–271.
[13] J. Marchese, M.C. Almandoz, M.A. Amaral, Una composición y procedimiento de preparación de pastas cerámicas para membranas de microfiltración, Argentinean Patent No. AR005203, 1999.
[14] M.C. Almandoz, Preparación y caracterización de capas activas de aluminosilicatos para microfiltración, Magister Thesis in Science of Surfaces and Porous Media, Universidad de San Luis, Argentina, 1998.
[15] J. Marchese, C.L. Pagliero, Characterization of asymmetric polysulfone membranes for gas separation, Gas Sep. Purif. 5 (1991) 215–221.
[16] J. Marchese, C. Almandoz, M. Amaral, L. Palacio, J.I. Calvo, P. Prádanos, A. Hernández, Fabricación y caracterización de membranas cerámicas tubulares para microfiltración, Bol. Soc. Esp. Cerám. Vidrio 39 (2000) 215–219.
[17] Standard Method for the Examination of Water and Wastewater, 19th ed., American Public Health Association/American Water Works Association/Water Environment Federation, Washington, DC, USA, 1995.